

## Epoxy–Diamine Thermoset/Thermoplastic Blends. 2. Rheological Behavior before and after Phase Separation

A. Bonnet, J. P. Pascault, and H. Sautereau\*

*Laboratoire des Matériaux Macromoléculaires-UMR CNRS 5627, Institut National des Sciences Appliquées, 20, Avenue A. Einstein, 69621 Villeurbanne Cedex, France*

Y. Camberlin

*Institut Français du Pétrole-Industrial Research and Development Center BP 3, 69390 Vernaison, France*

*Received November 12, 1998; Revised Manuscript Received May 17, 1999*

**ABSTRACT:** The phase separation process in a thermoplastic-modified epoxy system was studied using rheological dynamic analysis (RDA) and differential scanning calorimetry (DSC). Transmission electronic microscopy (TEM) was used to get direct representation of morphologies at different times during the phase separation process. The selected thermoset system was bisphenol A diglycidyl ether (DGEBA) cured with 4,4'-methylenebis[3-chloro,2,6-diethylaniline] (MCDEA) in the presence of various compositions of polyetherimide (PEI), 10–64 wt %. As rheology is a signature of connectivity, the rheological behavior at phase separation was found to be greatly dependent on the initial concentration of PEI. Experimental results showed that when PEI concentration was lower than 10–15 wt %, phase separation induced a rapid decrease of the viscosity. For concentrations close to the phase inversion composition, a rheological behavior characteristic of a bicontinuous morphology appeared with a strong dependence on frequency. When PEI concentration was higher than 30 wt %, phase separation led to a gradual increase in viscosity. A large interdependence between morphology and initial composition was exhibited. Modeling of the rheological behavior using kinetic parameters and the relationship between viscosity and mass average molar mass was in good agreement with the experimental results.

### Introduction

Thermoplastic (TP) and thermoset (TS) blends have been widely studied for two main applications: (i) toughness improvement of TS networks with high-performance ductile thermoplastics<sup>1</sup> and (ii) new processing routes for intractable high-temperature-resistant TP polymers, such as poly(phenylene ether), PPE.<sup>2</sup> For the first application, TP concentrations are generally lower than 20 wt %, and the phase separation process leads to a thermoset-rich continuous phase. For the second application, the TP concentration is higher than 30 wt %, and the phase separation process leads to a TP-rich continuous phase.<sup>2</sup>

Herein, we report the behavior of a blend of polyetherimide, (PEI) and a thermoset precursor (diglycidyl ether of bisphenol A, DGEBA, with 4,4'-methylenebis[3-chloro-2,6-diethylaniline], MCDEA), which were initially miscible. Riccardi et al.<sup>3</sup> found that the mixture exhibited a typical upper critical solution temperature (UCST) and was homogeneous at temperatures higher than 60 °C. Upon curing of this homogeneous solution, due to the molar mass increase of the thermoset precursor, a liquid–liquid phase separation occurred at a given extent of reaction,  $x$ . From this time, the two coexisting phases are viscoelastics and are changing in composition and extent of reaction versus curing time. Scattering techniques were able to determine the beginning of the phase separation at least at different scales. Girard-Reydet et al.<sup>4</sup> demonstrated that for initial quantities of PEI,  $\phi_{\text{PEI}}^0$  in the range 10–20 wt %, phase separation during epoxy–amine reactions proceeded by spinodal demixing (SD). Light transmission (LT) or light

scattering (LS) gave an estimation of the phase separation process. On the contrary, for  $\phi_{\text{PEI}}^0 \geq 30$  wt %, the second phase appeared through the nucleation and growth (NG) mechanism. In this case, small-angle X-ray scattering (SAXS) was able to observe the beginning of the phenomena before LT or LS.

Numerous studies have been devoted to investigate the viscosity of a polymer–polymer emulsion. Palierne<sup>5</sup> focused his attention on linear rheology of viscoelastic emulsion of two TP immiscible blends taking into account the interfacial tension and the relaxation times. Graebling and Muller<sup>6,7</sup> have used Palierne's model to determine the interfacial tension of TP/TP blends in melt. Ohta et al.<sup>8</sup> have performed an important work on the computer simulation of domain growth under steady shear flow, to predict the morphology evolutions, the change in viscosity, and normal force with the shear rate. Onuki<sup>9</sup> deal with initially homogeneous TP blends that phase separate during quench; blends are maintained close to the critical point composition, assuming that the viscosity of the two phases can be considered to be the same. Although different types of models exist in the literature to describe the viscosity evolution of immiscible TP–TP blends, any one is interested in a suspension like a TP in a reactive TS precursor, where the coexisting phases are changing continuously in composition with reaction time.

Part 1<sup>10</sup> reported the effects of phase separation on the rate of reaction. It was demonstrated that kinetic measurements were able to observe the beginning of the phase separation process. Modeling of the kinetics of the epoxy–amine reaction first in the homogeneous phase and second in each phase of a TS/PEI blend has been done. DSC, rheological, and dielectrical techniques

\* To whom correspondence should be addressed.

Table 1. Characteristics of the Blend Components

Name	Formula	Supplier
4,4' - methylenebis [ 3 - chloro 2,6- diethylaniline] <b>MCDEA</b> $M = 380 \text{ g.mol}^{-1}$		Lonza
diglycidyl ether of bisphenol A <b>DGEBA</b> $\bar{n}=0.15$ $M_n = 382.6 \text{ g.mol}^{-1}$		Ciba Geigy LY556
Polyetherimide <b>PEI</b> $M_n = 26000 \text{ g.mol}^{-1}$ $M_w = 50000 \text{ g.mol}^{-1}$ $T_g = 210^\circ\text{C}$		General Electric Ultem 1000

can also be used to monitor the phase separation process.<sup>11-15</sup> One advantage of these techniques is that they can be directly related to the processing. The aim of part 2 is to propose a much more detailed analysis of the phase separation process using rheological measurements.

## Experimental Section

**Materials.** The TS consisted of an epoxy prepolymer and a curing agent. The epoxy prepolymer used was a diglycidyl ether of bisphenol A liquid at room temperature and with a low degree of polymerization, DGEBA  $\bar{n} = 0.15$  (reference LY556 from Ciba Geigy). The curing agent was an aromatic diamine with a low reactivity, 4,4'-methylenebis(3-chloro-2,6-diethylaniline), MCDEA, supplied by Lonza. The diamine was used at the stoichiometric ratio of epoxy to amino hydrogen groups equal to 1.

The TP was polyetherimide, PEI Ultem 1000, supplied by General Electric. The chemical structures and characteristics of all materials are listed in Table 1.

Blends with low TP concentrations,  $\leq 20 \text{ wt } \%$ , were prepared in a two-stage process: TP was first dissolved at  $140^\circ\text{C}$  in the epoxy prepolymer, and the diamine was then added at  $90^\circ\text{C}$ .<sup>7</sup> Blends with concentration higher than  $30 \text{ wt } \%$  of TP (33, 48, and  $64 \text{ wt } \%$  of PEI) were prepared using a corotating twin-screw extruder in a one-stage process.<sup>16</sup>

**Measurements.** As explained in part 1,<sup>10</sup> high-performance liquid chromatography (HPLC) was employed to measure the extent of epoxy reaction,  $x$ . The HPLC measurements are a global measure so the epoxy conversion after phase separation will be noted  $\bar{x}$ . A Waters instrument was used with a low-pressure gradient, a 600 E solvent programmer, a U6k injector, a UV 86 detector set at  $254 \text{ nm}$ , and with a novopack C18 column ( $4 \mu\text{m}$ ). The solvent was a mixture of double-filtered water (A) and acetonitrile (B) (UV spectroscopy grade). The chromatographic separations were achieved by using a gradient program. First a gradient elution was carried out from 80 to 100 vol % acetonitrile (B) for 20 min, and then isocratic elution followed for 28 min, after which a gradient elution was effected from 100 to 80 vol % (B) for 32 min. The flow rate was  $1 \text{ mL/min}$  and the temperature  $20^\circ\text{C}$ . For PEI blends, the extraction of soluble products was conducted in two steps: first in dichloromethane at  $10 \text{ wt } \%$ , which was used to dissolve both PEI and epoxy copolymer, and then in acetonitrile at  $0.2 \text{ wt } \%$  to precipitate PEI. A complete extraction of residual epoxy-amine oligomers was then possible even if phase

separation had occurred. A  $20 \mu\text{L}$  aliquot of the sample solution was injected.

The gelation time was also obtained using HPLC measurements and was defined as the time at which the presence of an insoluble fraction was first observed.

The viscoelastic properties were measured by shear rheology. A Rheometrics dynamic analyzer (RDA II) was used. One geometry was chosen, namely, parallel plates with diameter 25 or 8 mm. The isothermal temperature was  $135^\circ\text{C}$ . The dynamic time sweep at a given temperature, pulsation ( $1 \text{ rad/s}$ ), and deformation ( $1\%$ ) was used in order to obtain steady state and thus ensure that measurements were performed under dynamic equilibrium conditions.

Differential scanning calorimetry (DSC7 Perkin-Elmer) was used to measure the glass transition temperature,  $T_g$  (onset value), of the different samples. For  $T_g$  measurements a heating rate of  $10^\circ\text{C/min}$  was used.

Morphologies were studied by transmission electron microscopy (TEM) using a JEM-200CX. Ultrathin sections were obtained at room temperature. A natural contrast existed between the two phases when a  $80 \text{ kV}$  accelerating voltage was used. The mean particle size  $\bar{D}$ , the fraction of dispersed phase, and the number of particles per unit area were measured using an image analysis software, PCI3, developed in our lab.

## Results and Discussion

**Influence of PEI Concentration on the Rheological Behavior at Phase Separation.** As mentioned in the Introduction, the PEI concentration has a strong influence on both the mechanism of the phase separation process<sup>9</sup> and the final morphologies. Mean diameters,  $\bar{D}$ , of dispersed particles given by TEM analysis are presented in Figure 1 after a full cure (7 h at  $220^\circ\text{C}$ ). For initial PEI concentration,  $\phi_{\text{PEI}}^0 \leq 10 \text{ wt } \%$ , the continuous phase was the epoxy-amine-rich one ( $\alpha$  phase), and the mean diameter of the TP-rich particles was increased with PEI content. For  $\phi_{\text{PEI}}^0 \geq 30 \text{ wt } \%$  the continuous phase was the TP-rich one ( $\beta$  phase), and the mean diameter of the epoxy-rich particles was decreased with epoxy content. Between 10 and  $30 \text{ wt } \%$  more or less well-defined bicontinuous structures were formed, and it was not possible to give a mean diameter value.

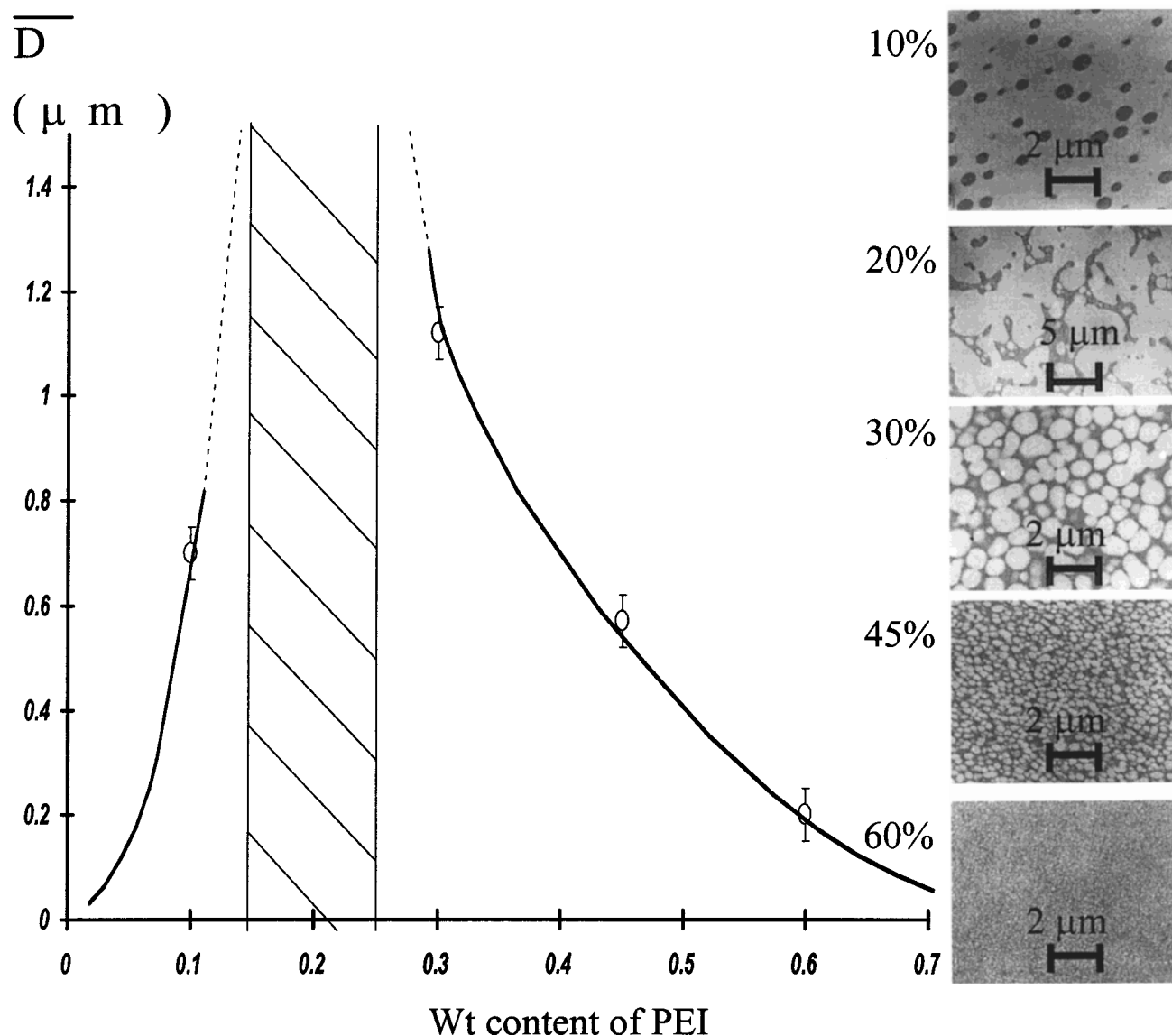


**Figure 1.** Mean particle diameter (and dispersion) as a function of the blend composition,  $\phi_{PEI}^0$ . The samples have been cured at 135 °C up to the vitrification of the matrix (during 5 h) and postcure at 220 °C (during 7 h). The micrographs are taken after the postcure step.

In Figure 2 there are three micrographs of the morphologies of the fully cured samples (220 °C, during 7 h) and for three different concentrations: 10, 20, and 33 wt %. This clearly shows the bicontinuous structure at 20 wt % and the inverted morphology at 33 wt %. But the main aim of Figure 2 is to illustrate the rheological behavior of the blend. For a clearer explanation we have plotted the complex viscosity increase,  $\eta^*$ , upon curing for the three different  $\phi_{PEI}^0$  on the same arbitrary curing time (or conversion) scale where  $t_{cp}$  is the reference of the scale. The measurements were done at a low frequency, 1 rad/s. The final curing time for each blend at 135 °C is 350 min.

At the beginning of the reaction, the homogeneous blend behaved as either a semidilute polymer solution or a standard polymer melt, depending on the PEI concentration. When phase separation occurred,  $\eta^*$  increases or decreases abruptly, depending on the PEI concentration. Dual measurements<sup>12</sup> demonstrated that this point coincided with the cloud point (CP) observed by light transmission.

Rheology is a signature of connectivity. For this reason for low PEI concentrations,  $\phi_{PEI}^0 \leq 10$  wt %, the

phase separation process was followed by a rapid decrease in viscosity. This was due to the initially dissolved highly viscous PEI component separating from the epoxy-rich matrix. On the contrary, when PEI concentration was high enough to ensure a continuous TP-rich phase up to the end of the phase separation process ( $\phi_{PEI}^0 = 33$  wt %, for example), the onset of phase separation was accompanied by a gradual increase in viscosity.

For  $\phi_{PEI}^0 = 20$  wt % the behavior was more complex. In the beginning of the phase separation process a gradual increase in viscosity occurred due to the formation of a bicontinuous structure. But after some minutes, a decrease of  $\eta^*$  was observed which can be explained by the destruction of the bicontinuous structure and the reappearance and behavior of an epoxy-rich matrix. The amplitude of the obtained peak was found to be dependent on the frequency used for the measurement.

After this liquid-liquid transition, the rheological behavior was one of a two-phase system. Other rheological events, like vitrification of the  $\beta$  phase, can be detected and are going to be discussed for one blend composition.

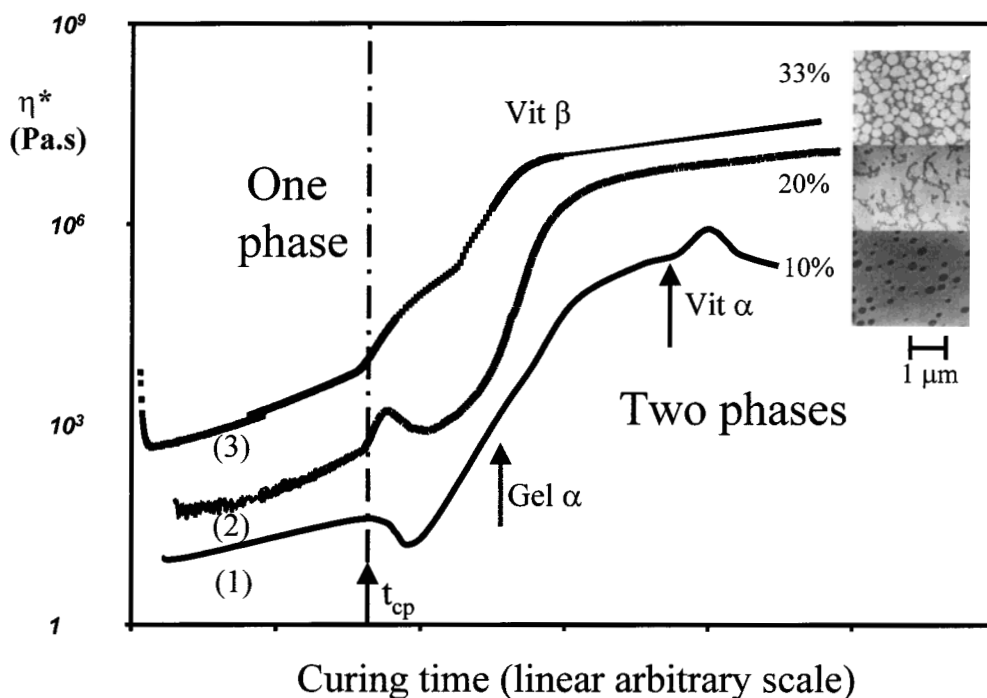


**Figure 2.** Influence of PEI concentration on the rheological behavior: (1) 10 wt %, (2) 20 wt %, and (3) 33 wt %. TEM micrographs illustrate the final morphologies obtained at  $T_i = 135^\circ\text{C}$  after 5 h and postcure at  $220^\circ\text{C}$  (during 7 h).

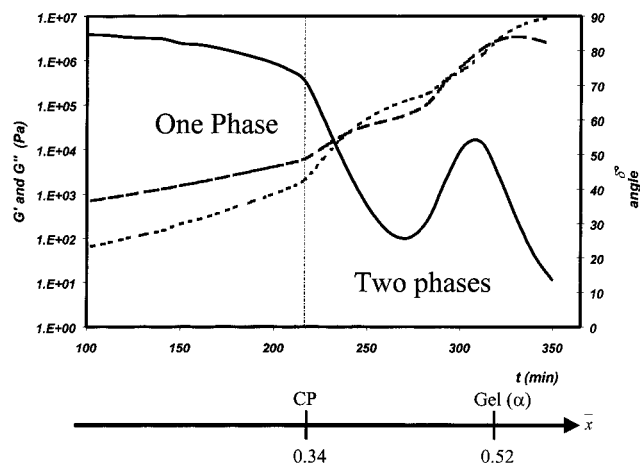


**Figure 3.** Rheological behavior of a blend with 33 wt % of PEI upon curing at  $T_i = 135^\circ\text{C}$ : (---) modulus of conservation  $G'$ ; (---) modulus of loss  $G''$ ; (—) angle  $\delta$ ; pulsation 1 rad/s.

**Relation between Rheological Behavior and Morphological Evolutions.** Figure 3 details the rheological results obtained versus a real time/conversion scale in the case of the blend with 33 wt % PEI. In this case when phase separation occurred, the behavior of the TP-rich  $\beta$  phase, richer in PEI than the initial homogeneous phase, dominated and the  $\delta$  angle decreases and the modulus of conservation  $G'$  and the modulus of loss  $G''$  increase. After the cloud point, CP, the behavior is one of a two-phase system but complicated by the fact that many parameters are changing such as the size, volume fraction, and number of dispersed particles, but also the composition and epoxy conversion of both phases and the extent of reaction in each phase.

Figure 4 depicts the evolution of  $T_g$  versus curing time/conversion for a blend with 33 wt % PEI. For this experiment, 12 samples are heated at  $135^\circ\text{C}$  in a thermo-regulated oil bath, and samples are taken and quenched in nitrogen for different times of cure. Initially

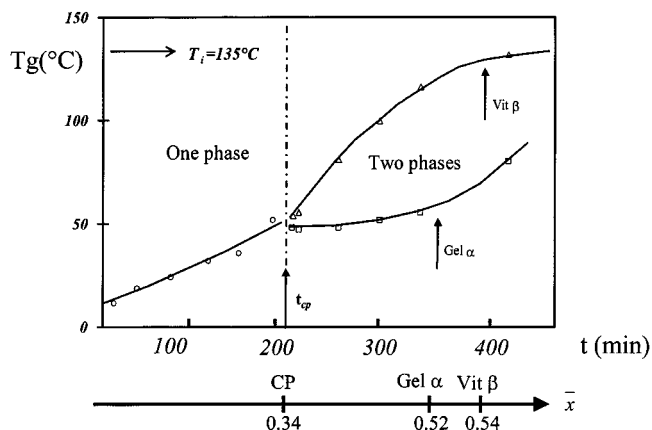


**Figure 4.**  $T_g$  evolution versus curing time for the blend with 33 wt % of PEI at  $135^\circ\text{C}$ .

the homogeneous blend has one  $T_g$ , which can be obtained from the  $T_g$  of the TP and the  $T_g$  of the epoxy-amine copolymer through the Couchman equation.<sup>17</sup> The temperature at which the DGEBA-MCDEA copolymer gels and vitrifies,  $_{\text{gel}}T_g$ , has been determined previously to be  $54^\circ\text{C}$ .<sup>18</sup> Because the curing was done at a higher temperature,  $T_i = 135^\circ\text{C}$  than  $_{\text{gel}}T_g$ , after the cloud point the dispersed  $\alpha$  phase is a liquid and is going to gel first and then to vitrify. In the case of a blend, this sol-gel transition is difficult to observe on the rheological experimental curves (Figure 3). It was determined by the appearance of an insoluble fraction during HPLC measurements,  $\bar{x}_{\text{gel}} = 0.52$ .

After the cloud point for such PEI concentration, 33 wt %, the  $\alpha$  phase can be observed by TEM analysis as forming spherical nodules dispersed in the TP-rich matrix (Figure 1). Evolutions of the size distribution and mean diameter,  $\bar{D}$ , of dispersed particles versus curing time or conversion are given in Figures 5 and 6. Using SAXS measurements, the beginning of the phase separation process can be estimated at  $x = 0.20\text{--}0.25$ .<sup>4</sup> Up



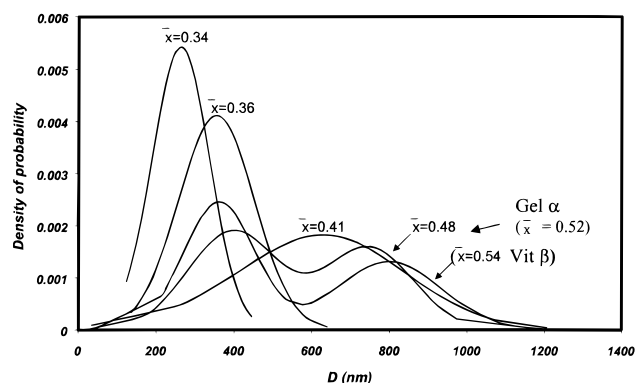


**Figure 5.** Evolution of the diameter distribution of the dispersed particles upon curing time at  $T_i = 135\text{ }^{\circ}\text{C}$  for the blend with 33 wt % of PEI; TEM final morphology ( $\bar{x} = 0.54$ ),  $\bar{D}$  = mean diameter ( $\mu\text{m}$ ).

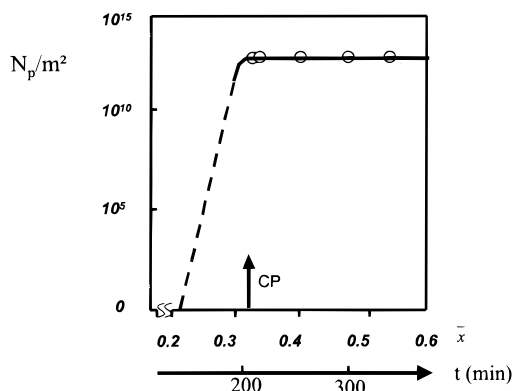


**Figure 6.** Evolution of the number  $N_p$  of dispersed particles/ $\text{m}^2$ . Same experimental conditions as in Figure 4.

to the cloud point the mean diameter (Figure 5) and the number (Figure 6) of epoxy rich dispersed particles increased very rapidly. After the cloud point, the number of particles,  $N_p$ , practically stabilized, which was well before both gelation of the  $\alpha$  phase ( $\bar{x}_{\text{gel}} = 0.52$ ) and vitrification of the  $\beta$  phase ( $\bar{x} \approx 0.54$ ). This behavior meant that the nucleation step was finished. During the same time the growth of the particles continued until vitrification of the  $\beta$  phase. But in the vicinity of vitrification of the  $\beta$  phase, a second population of dispersed particles appears. At that time, diffusion of the epoxy-amine copolymer is more and more difficult in the high viscous medium, and phase separation occurs more locally.

**Modeling of the Viscosity Evolutions upon Curing.** Having established the phenomenological effects observed during the phase separation process, their quantitative evaluations by modeling the melt viscosity  $\eta^*$  of a reactive blend with 33 wt % PEI during its cure are going to be presented. Three stages can be distinguished.

(i) Before phase separation, the viscosity was the one of a homogeneous mixture.

It can be described with the help of the blend composition and the viscosities of the two components. The viscosity of the homogeneous solution increased due to the reaction of the epoxy-amine precursor.

Equation 1 gives the viscosity of a blend of two miscible polymers.<sup>19</sup>

$$\eta^* = \{\eta^*_{\text{DGEBA}}\}^{\phi_{\text{DGEBA}}} + \{\eta^*_{\text{PEI}}^{\text{fit}}\}^{\phi_{\text{PEI}}} \quad (1)$$

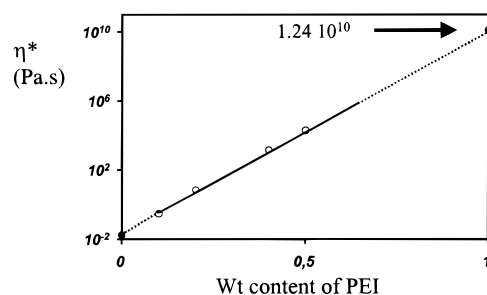


**Figure 7.** Initial viscosity as a function of the nonreactive blend composition DGEBA  $\bar{n} = 0.15/\text{PEI}$  at a constant temperature ( $135\text{ }^{\circ}\text{C}$ ): (○) experimental points, (●) estimated points.

This equation requires an estimate of a hypothetical viscosity of pure PEI at  $135\text{ }^{\circ}\text{C}$  in the liquid state. For this purpose different nonreactive homogeneous blends, with DGEBA  $\bar{n} = 0.15$  alone and PEI were prepared, and the viscosity was measured at  $135\text{ }^{\circ}\text{C}$ . Blends with PEI content  $> 80\text{ wt } \%$  had a  $T_g$  above  $135\text{ }^{\circ}\text{C}$  and were therefore not studied. In eq 1 the superscript “fit” serves as a reminder that PEI viscosity is a fitting value only. For  $\eta_{\text{DGEBA}}$ , the measured value is  $0.02\text{ Pa}\cdot\text{s}$ . Figure 7 depicts the viscosity of the hypothetical “supercooled” melt of PEI;  $\eta_{\text{PEI}}^{\text{fit}}$  was determined equal to  $1.24 \times 10^{10}\text{ Pa}\cdot\text{s}$ . This value will be used in the next calculation.

The increase of viscosity due to the epoxy-amine copolymer,  $\eta_{\text{ea}}$  can be correlated to the copolymer mass average molar mass,  $\bar{M}_w$ :

$$\eta_{\text{ea}} = K(g\bar{M}_w)^a \quad (2)$$

In this relation  $K$  was a function of temperature,  $a$  was generally found to be equal to 3.4,<sup>20</sup>  $\bar{M}_w$  had to be calculated, and  $g$  was the ratio of the gyration radius of a branched macromolecule to the gyration radius of a linear macromolecule having the same molar mass with

$$g = \frac{1 - 3rx^2}{2rx^2} \ln \frac{1 - rx^2}{1 - 3rx^2} \quad (3)$$

where  $r = [\text{amino hydrogen groups}]/[\text{epoxy groups}]$  is the stoichiometric ratio and  $x$  the conversion of epoxy groups.

To calculate  $\bar{M}_w$  evolution during thermoset reaction, the Macosko-Miller<sup>21</sup> equation was used.

$$\bar{M}_w = \frac{[1 + x(4x - X + 1)]M_{A_4}^2 + 2[1 + x(X - 1)]M_{E_2}^2 + 8xM_{A_4}M_{E_2}}{(M_{A_4} + 2M_{E_2})[1 - x(X - 1)]} \quad (4)$$

As the reaction proceeded with  $A_4$  moles of MCDEA monomer and  $E_2$  moles of DGEBA, the different parameters were defined as

$$\alpha_i = \frac{A_{4,i}}{\alpha_0}; \quad x = \frac{\sum_{i=0}^4 i\alpha_i}{4}; \quad X = \frac{\sum_{i=0}^4 i^2\alpha_i}{4x}$$

$M_{A_4}$  is the molar mass of diamine monomer,  $A_{4,i}$  is the moles of diamine monomer with  $i$  reacted sites,  $M_{E_2}$  is molar mass of monomer epoxy,  $a_0$  is moles of initial

amino hydrogen group,  $x$  is the conversion of amino groups which was equal to the conversion of epoxy groups if there were no etherification, and  $X$  is the weight-average extent of reaction.

$\alpha_i$  was a function of  $p$  and  $q$ ,  $p = 2/(2 - n)$ , and  $q = (2 + n)/4$ , where  $n$  was the ratio of the rate constant of secondary to primary amino groups;  $n = k_2/k_1$  was equal to 0.65<sup>18</sup> for MCDEA.

As we were able to calculate  $\bar{M}_w$  during the reaction, the changing of melt viscosity can be described before phase separation as a function of time.

$$\eta_{(t)\text{blend}}^* = \{K(g_{(t)}\bar{M}_{w(t)})^a\}^{\phi_{\text{ea}}} + \{\eta_{\text{PEI}}^*\}^{\phi_{\text{PEI}}} \quad (5)$$

(ii) After phase separation this viscosity became the one of a suspension of dispersed particles ( $\alpha$ ) in a matrix ( $\beta$ ).

As explained in the Introduction, different types of modeling exist in the literature for suspensions, but all these studies focused on nonreactive immiscible TP/TP blends, for which the phase compositions are constants with time. Our case is more complex as the extent of reaction and compositions are changing with time. The use of Palierne's model for example suggests the knowledge of the evolution with conversion and composition of the interfacial tension between the two phases and the phases' relaxation times. All these parameters are not accessible during cure of our TS/TP blend and should be taken as adjustable parameters. For this reason we prefer to use in a first approximation the Einstein equation<sup>22</sup> (even if we know that Einstein equation does not take into account viscoelastic effects) which writes that the suspension viscosity is mainly governed by the matrix viscosity evolution and the quantity of dispersed phase:

$$\eta_{\alpha,\beta(t)} = \eta_{\beta(t)}(1 + 2.5K_{\text{e}(t)}\phi_{\alpha(t)}) \quad (6)$$

$\phi_{\alpha(t)}$  was the volume fraction of the dispersed  $\alpha$  phase, and  $K_{\text{e}(t)} = 0.4 + \lambda_{(t)}/1 + \lambda_{(t)}$  with  $\lambda_{(t)}$  the ratio of the viscosities of the  $\alpha$  and the  $\beta$  phases.

Knowing the parameters  $\eta_{\beta(t)}$ ,  $\phi_{\alpha(t)}$ , and  $\lambda_{(t)}$  it was easy to calculate the viscosity  $\eta_{\alpha,\beta(t)}$ . But in this case, all the parameters were changing with reaction times. As previously noted, the viscosity of the epoxy–amine, ea, copolymer was a function of  $\bar{M}_w$ , but now the reaction rates were different in  $\alpha$  and  $\beta$  phases. To know  $\eta_{\text{ea},\alpha}$  and  $\eta_{\text{ea},\beta}$  it was necessary to use  $\bar{M}_{w,\alpha}$  and  $\bar{M}_{w,\beta}$  (eq 2), which meant knowing  $x_\alpha$  and  $x_\beta$ . As in part 1,<sup>10</sup> a rough estimation of the parameters  $x_\alpha$  and  $x_\beta$  was made with measurements of  $T_g$  and  $\Delta C_p$  (heat of capacity change at  $T_g$ ) of each phase (Figure 4 for  $T_g$  measurements,  $\Delta C_p$ 's evolution is not given here).

Using the Couchman equation<sup>17</sup> and by considering that each phase was homogeneous, it was possible to write for  $\alpha$  and  $\beta$  phases:

$$\ln T_{g(\alpha)} = \frac{M_{1(\alpha)}\Delta C_{p1(\alpha)} \ln T_{g1(\alpha)} + [1 - M_{1(\alpha)}]\Delta C_{p2} \ln T_{g2}}{M_{1(\alpha)}\Delta C_{p1(\alpha)} + [1 - M_{1(\alpha)}]\Delta C_{p2}} \quad (7)$$

$$\ln T_{g(\beta)} = \frac{M_{1(\beta)}\Delta C_{p1(\beta)} \ln T_{g1(\beta)} + [1 - M_{1(\beta)}]\Delta C_{p2} \ln T_{g2}}{M_{1(\beta)}\Delta C_{p1(\beta)} + [1 - M_{1(\beta)}]\Delta C_{p2}} \quad (8)$$

$T_g$  of component 1 (epoxy–amine) was changing with mean conversion  $\bar{x}$ , while  $T_g$  of component 2 (PEI) was

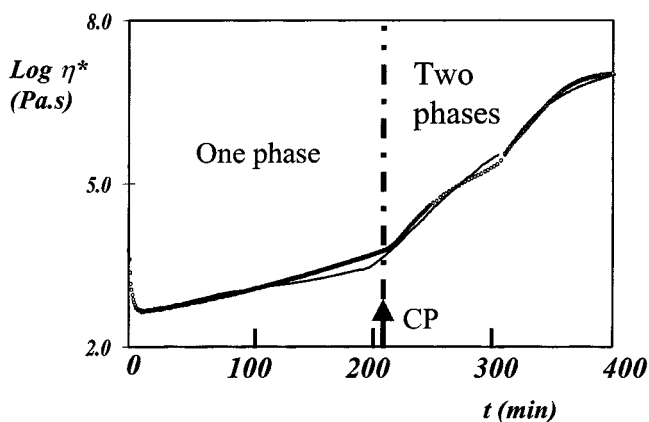


**Figure 8.** Simulation of the evolution of viscosity during the cure at 135 °C of a reactive blend DGEBA ( $\bar{n} = 0.15$ )–MCDEA with 33 wt % of PEI: (○) experimental points, (—) modeling.

constant.  $M_1$  was the weight ratio of component 1 (epoxy–amine copolymer) in the  $\alpha$  phase,  $M_{1(\alpha)}$ , or in the  $\beta$  phase,  $M_{1(\beta)}$ .

Then considering again that the matrix ( $\beta$ ) and the dispersed ( $\alpha$ ) phases were homogeneous, eq 1 can be applied at different curing times or epoxy conversions.

$$\eta_{\alpha(t)}^* = \{K(g_{(t)}(\bar{M}_{w\alpha(t)})^a\}^{\phi_{\text{ea}\alpha(t)}} + \{\eta_{\text{PEI}}^*\}^{\phi_{\text{PEI}\alpha(t)}} \quad (9)$$

$$\eta_{\beta(t)}^* = \{K(g_{(t)}(\bar{M}_{w\beta(t)})^a\}^{\phi_{\text{ea}\beta(t)}} + \{\eta_{\text{PEI}}^*\}^{\phi_{\text{PEI}\beta(t)}} \quad (10)$$

Calculations were made for the blend with 33 wt % PEI. The  $\phi_\alpha$  values were also obtained by TEM (Figures 5 and 6) and can be used to confirm the calculations of  $x_\alpha$  and  $x_\beta$  from eqs 7 and 8 and mass balance (cf. part 1<sup>10</sup>).

Of course, this modeling can be made using the Einstein equation only before gelation of the  $\alpha$  phase.  $K$  (eq 2) was an adjustable parameter. Before and after phase separation,  $K$  was found to be equal to the same value, 4.26.  $K$  would be certainly different with another initial amount of PEI or for another curing temperature.

(iii) In the later stages of the reaction, for initial PEI concentration equal to 33 wt %,  $\beta$  phase behavior dominated.

Therefore, in the vicinity of its vitrification, from  $t = 310$  min, time corresponding to the maximum of the relaxation peak, the WLF relation has to be used:<sup>23</sup>

$$\ln \eta_{(t)}^* = \ln \eta_{\text{ref}}^* + \frac{C_1 + (T_{g(t)} - T_{\text{ref}})}{C_2 + (T_{g(t)} - T_{\text{ref}})} \quad (11)$$

where  $C_1$  and  $C_2$  are constants and  $T_{\text{ref}}$  is a reference appropriate for a particular polymer.  $\eta_{(t)}^*$  and  $\eta_{\text{ref}}^*$  are the viscosity at  $T_{g(t)}$  and  $T_{\text{ref}}$ . For modeling  $T_{\text{ref}}$  was equal to 122 °C.  $\eta_{\text{ref}}^*$  was equal to  $1.207 \times 10^7$  Pa.s.  $C_1$  and  $C_2$  were adjustable parameters and are respectively found equal to 3.5 and 55 °C. They cannot be compared to the universal ones because of the presence of the dispersed curing  $\alpha$  phase.

The results of the overall simulation for the three stages (i), (ii), and (iii) are finally given in Figure 8. The goal of the modeling was to quantify the effect of the different parameters. This modeling was a rough estimation, but it helped us to understand the influence of the different transitions and transformations, which

occur during the cure. Before phase separation we observed that the evolution of viscosity was mainly due to the extent of the epoxy-amine reaction. After phase separation, we noted that the behavior of the blend was mainly due to the evolution of the composition of the  $\beta$  phase. When vitrification of this phase occurs, the viscosity of the suspension could be described essentially by a WLF relation, showing that the main effect was the concentration increase of TP component in the  $\beta$  phase ( $T_g$  increase).

## Conclusion

A direct relationship between morphology and initial composition was exhibited. Phase separation process in TS/TP blends was monitored using rheological measurements. Depending on the initial concentration of thermoplastic, different behaviors were observed. For thermoplastic concentration  $\leq 15$  wt %, a rapid decrease in viscosity was observed after phase separation due to the formation of a continuous  $\alpha$  phase. For thermoplastic concentration close to phase inversion a phenomenon with a peak amplitude was observed as a function of frequency. This was due to the percolation in the earlier time of phase separation of the thermoplastic-rich phase. For thermoplastic concentrations equal to and higher than 30 wt %, the phase separation process induced a gradual increase in viscosity. Rheological behavior of  $\beta$  phase was found to be the main parameter influencing the final morphology. Microscopy and thermal measurements were used for a blend with initially 33 wt % of PEI to model the rheological behavior of the heterogeneous blend by taking into account the changes in phase compositions, in morphology, and in extent of reaction before and after phase separation. This simulation helped us to understand the various phenomena occurring during cure and provided an insight into the main parameters influencing the rheological behavior.

**Acknowledgment.** The contributions of H. Perier Camby (reactive extrusion) and I. Bornard (transmission electron microscopy) are gratefully acknowledged.

## References and Notes

- (1) Williams, R. J. J.; Rozenberg, B. A.; Pascault, J. P. Reaction-induced phase separation in modified thermosetting polymers. *Adv. Polym. Sci.* **1996**, *128*, 95.
- (2) Venderbosch, R. W.; Meijer, H. E. E.; Lemstra, P. J. *Polymer* **1995**, *36*, 2903.
- (3) Riccardi, C. C.; Borrajo, J.; Williams, R. J. J.; Girard-Reydet, E.; Sautereau, H.; Pascault, J. P. *J. Polym. Sci., Polym. Phys.* **1996**, *34*, 349.
- (4) Girard-Reydet, E.; Sautereau, H.; Pascault, J. P.; Keates, P.; Navard, P.; Thollet, G.; Vigier, G. *Polymer* **1998**, *39*, 2269.
- (5) Paliarne, J. F. *Rheol. Acta* **1990**, *29*, 204.
- (6) Graebing, D.; Muller, R. *Colloids Surf.* **1991**, *55*, 89.
- (7) Graebing, D.; Muller, R. *J. Rheol.* **1990**, *34*, 193.
- (8) Otha, T.; Nozaki, H.; Doi, M. *J. Chem. Phys.* **1990**, *93*, 2664.
- (9) Onuki, A. *Phys. Rev. A* **1987**, *35*, 5149.
- (10) Bonnet, A.; Pascault, J. P.; Sautereau, H.; Taha, M.; Camberlin, Y. *Macromolecules* **1999**, *32*, 8517.
- (11) Venderbosch, R. W. Ph. D Thesis, ISBN 90-386-0176-X, 1995; Chapter 7, p 135.
- (12) Vinh-Tung, C.; Lachenal, G.; Chabert, B.; Pascault, J. P. In *Toughened Plastics II: Novel Approches in Science and Engineering*; Riew, C. K., Kinloch, A. J., Eds.; *Adv. Chem. Ser.* **1994**, *252*, 59.
- (13) Poncet, S.; Boiteux, G.; Pascault, J. P.; Sautereau, H.; Seytre, G.; Rogozinski, J.; Kranbuehl, D. *Polymer* **1999**, *40*, 6811.
- (14) Swier, S.; Van Mele, B. Polymer Network Preprint P12, Trondheim, 1998.
- (15) Alig, I.; Jenninger, W. *J. Polym. Sci., Part B* **1998**, *36*, 2461.
- (16) Maazouz, A.; Becu, L.; Merle, G.; Taha, M. *J. Appl. Polym. Sci.*, to be published.
- (17) Couchmann, P. R. *Macromolecules* **1978**, *11*, 1156.
- (18) Girard-Reydet, E.; Riccardi, C. C.; Sautereau, H.; Pascault, J. P. *Macromolecules* **1995**, *28*, 7599.
- (19) Couchman, P. R. *J. Appl. Polym. Sci.* **1996**, *60*, 1057.
- (20) Zimm, B. H.; Stockmayer, W. H. *J. Chem. Phys.* **1949**, *17*, 1301.
- (21) Macosko, C. W.; Miller, D. R. *Macromolecules* **1980**, *13*, 1063.
- (22) Einstein, A. *Ann. Phys.* **1911**, *24*, 591.
- (23) Mijovic, J.; Chee Hung, L. *J. Appl. Polym. Sci.* **1989**, *37*, 889.

MA981755H